The Helmholtz Resonator

Nico Deshler*
Physics Department, University of California Berkeley.
(Dated: May 9, 2021)

This study explores the relationship between the resonance frequency of a Helmholtz resonator and two of its geometric parameters: the cavity volume and the neck length. Spectrograms of the audio signal generated by different resonator geometries are collected and used in a spectral analysis of the resonant frequencies. Power law fits of the resonance frequencies measured for different cavity volumes and different effective neck lengths yield $\nu_r(V) = 4.04 \cdot V^{-0.50}$ and $\nu_r(L_e) = 18.46 \cdot {L_e}^{-0.74}$ respectively. Theoretical predictions are in greater agreement with the power law relationship found for the cavity volume than for the neck length. An analysis of the measurement error and the damping (Q factor) of the Helmholtz resonator are also provided.

Key Terms: Helmholtz Resonance Frequency, Acoustic Spectral Analysis, Helmholtz Resonator Neck Length, Helmholtz Resonator Volume

I. INTRODUCTION

Helmholtz resonators offer an accessible experimental platform for exploring the physics of acoustic resonance. These objects can be generally described as a rigid hollow enclosure with a single opening. Typically, the enclosure is equipped with a hollow neck with the opening at one end [Figure 1]. Blowing air over the opening causes the air column within the neck to oscillate, creating sound. The structural simplicity of Helmholtz resonators explains their ubiquitous presence among household items. Bottles, cups, and bowls, as well as instruments like acoustic guitars and pan flutes are all examples of Helmholtz resonators. Even a moving car with an open window can be classified as a Helmholtz resonator.

Historically, these objects were of interest to musicians as they provided a means of passively amplifying their instruments. Likewise, scientists like Lord Rayleigh have found them fascinating for understanding the physics of sound propagation [1]. These structures even appear in nature. Certain bird species use tree hollows to amplify their songs while certain cricket species have evolved anatomically with resonators to amplify mating calls [2]. Today Helmholtz resonators are used in the exhaust manifold of combustion vehicles for attenuating the noise of the engine [3]. There is also ongoing research on how to apply the theory of Helmholtz resonators to aircraft for similar noise purposes [4].

This work explores the effect of varying two geometric features of the Helmholtz Resonator: (a) The volume of the cavity, and (b) the length of the neck. The acoustic resonance frequency of the device is measured against these geometric parameters.

* nico.deshler@berkeley.edu

II. THEORY

The Helmholtz resonator can be modelled as a block-spring system. The volume of the air column in the neck is the mass $m = \rho(AL)$ [Figure 2] while the periodic compression of this air column behaves like a spring and produces sound. The natural oscillation frequency for a block-spring system with spring constant k is known to be

$$\nu_r = \frac{1}{2\pi}\sqrt{\frac{k}{m}} \tag{1}$$

Treating air as an ideal gas and acoustic resonance as an adiabatic process [see derivation in Appendix A], the resonance frequency of a Helmholtz resonator is,

$$\nu_r = \frac{c}{2\pi}\sqrt{\frac{A}{VL_e}} \tag{2}$$

where c is the speed of sound in air (343 m/s at STP), A is the area of the opening, V is the volume of the resonator, and L_e is the effective neck length,

$$L_e = L + \alpha\sqrt{A} \tag{3}$$

Here L is the neck length and α is a constant related to the geometry of the opening. In previous work by Lord Rayleigh and William Strutt [1], the correction factor of a cylindrical neck with a flanged circular opening is found analytically to be $\alpha = \frac{16}{3\pi^{3/2}} \approx 0.96$. All configurations of the Helmholtz resonator used in experiments feature a circular opening.

III. MATERIALS AND METHODS

The Helmholtz resonator used in this study was a glass Hornitos Tequila bottle which was chosen for its simple shape and loud resonance characteristics. The cavity of

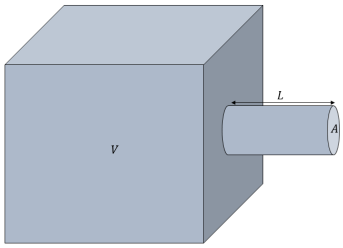

FIG. 1. A schematic of a typical Helmholtz resonator and its relevant geometric parameters.

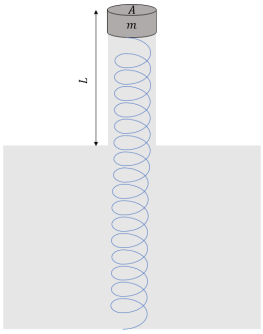

FIG. 2. A diagram of the Helmholtz resonator modelled as a mass on a spring.

the resonator approximates a rectangular prism and the neck is a cylinder that leads to a flanged circular opening. The neck has length $L = 42.8 \pm 1$ mm and the opening has diameter $D = 18.5 \pm 1$ mm. To stimulate resonance, an experimenter orally blew over the opening of the glass bottle. Simultaneously, a spectrogram of the acoustic signal was captured on an iPhone 6 using the commercially available application, SpectrumView. All experimental measurements were conducted in a sauna (at STP) which offered an environment with good sound isolation to prevent echo and suppress background noise. The aforementioned steps provide a basic overview of the experimental procedure and relevant materials. Next we describe how the geometric parameters of the resonator were modulated.

A. Modulating the Resonator Volume

The total volume of the empty resonator cavity was measured to be 750 ± 1 mL by filling the bottle to the base of the neck with water. To change the volume to a desired level, water was either added or removed from the cavity and left on a flat surface to settle. As an incompressible fluid, water offers a simple way of modulating the volume while preserving the rigidity of the active cavity. The cavity volumes explored in this study range from $0 - 750$ mL. Note that in the case of 0 volume (i.e. the bottle is filled until the base of the neck), the Helmholtz resonator transitions in regime. The resonator can no longer be thought of as a cavity with a neck. Instead, the neck itself becomes the cavity making the resonator a pipe with one opening. Therefore, we do not expect the resonance frequency at zero cavity volume to be comparable to the regime of the original bottle anatomy. For this reason, the zero volume measurements are omitted in the analysis.

FIG. 3. Experimental materials and the Helmholtz resonator shown with (top-left) no extension, (top-right) one extension, (bottom-left) two extensions, (bottom-right) three extensions. The volume of the resonator was adjusted by filling the bottle with water to desired levels.

B. Modulating the Resonator Neck Length

The neck length of the resonator was increased by stacking cylindrical copper extensions on top of the bottle opening. The extensions were tapered at one end to enable pressure-fitting one extension into the next to form a rigid stack. The untapered end was chosen to match the diameter of the bottle opening. However, the tapered end constricts to a smaller diameter and therefore modified the inner geometry of the neck. With the extensions, the inner geometry of the neck departs somewhat from a smooth cylinder and acquires ribbed features. Nevertheless, the aperture of the resonator remains constant across experimental configurations.

TABLE I. Copper extension Diameters

with Taper	**without Taper**
19.8 ± 0.5 [mm]	15.9 ± 0.5 [mm]

C. SpectrumView Configuration and Calibration

The measurements collected in this study are spectrograms of the audio signal produced by the Helmholtz resonator [Figure 4]. These spectrograms were recorded using the SpectrumView application available for iPhone. The application was configured to acquire samples of the audio signal at 16,000 Hz. By the Nyquist Theorem this provided us with a frequency range of 0-8000 Hz. To prevent aliasing, SpectrumView defaults to low-pass filtering the audio signal with a Blackman window [see Appendix A Equation B1 and Reference [5]]. This window exhibits a low-pass threshold at $0.12 \cdot \nu_{max}$ where $\nu_{max} = 8000$ Hz is the upper-limit of the frequency range. Therefore, the filter attenuates all frequencies above 960 Hz. All the resonance frequencies used in our analysis fall below this threshold and therefore are not attenuated.

To ensure the fidelity of our spectral analyzer, the SpectrumView application was calibrated by playing a sine wave at 750 Hz through a laptop speaker and asserting agreement with the recorded spectrogram. A spectrogram of the ambient noise in our test environment was also collected to verify that the background signature was negligible.

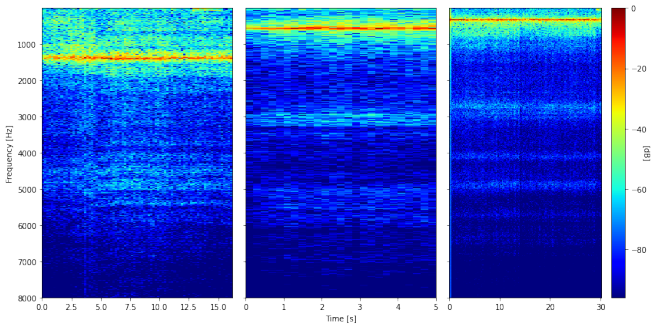

FIG. 4. Three examples of spectrogram measurements captured with SpectrumView. As a pre-processing step, the measurement time intervals for each spectrogram were cut and spliced together to remove moments in which the experimenter was between breaths.

IV. ANALYSIS

A. Spectral Analysis and Resonance Frequencies

To analyze how volume and neck length affects the resonance frequency of the Helmholtz resonator, each measured spectrogram was converted into a spectral power distribution by averaging the spectrogram over time. The resonance frequencies are then easily identified from the peaks of the spectral power curves.

Figure 5 shows the spectral power distributions of the resonator for different cavity volumes with the neck length held constant at 42.8 mm. Figure 6 shows the

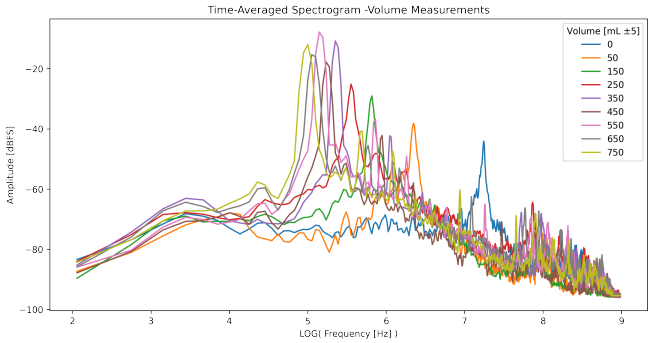

FIG. 5. Spectral power distributions for the Helmholtz resonator configured with different volumes. The curves were constructed by time-averaging the raw spectrograms acquired for each cavity volume. Upon close inspection, secondary peaks appear at higher frequencies suggesting the presence of harmonics.

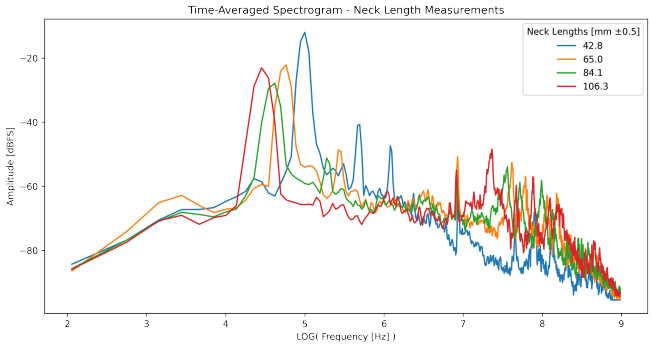

FIG. 6. Spectral power distributions for the Helmholtz resonator configured with different neck lengths.

spectral power distributions produced by the resonator for different neck lengths with the cavity volume held constant at 750 mL. These graphs are plotted on a log axis to make the peaks more visually distinguished.

Form these spectral power distributions, we parse the resonance frequencies corresponding to the volume and neck length modulation experiments. These frequencies are plotted against their respective geometric parameter in Figures 7 and 8. From equation 2 we see that the resonance frequency varies proportionally to the inverse square root of the volume V and of the effective neck length L_e. Guided by this theoretical background, we apply a curve fit to a power law of the form $f(x) = Bx^b$ where B, b are the fit parameters and $x \in \{V, F_e\}$ is the geometric parameter modulated in experiment.

B. Error Analysis

Several considerations are important to quantifying the error in the resonance frequency given the experimental techniques employed in this study. Let us first investigate the *precision error* introduced by the

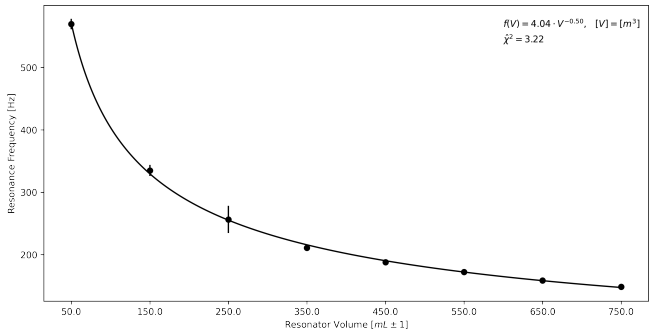

FIG. 7. Resonant frequencies measured for different resonator volumes. The curve fit parameters [shown] demonstrates good agreement with the theoretically expected power law relationship. It exactly matches the theoretical prediction for the exponent $b = -1/2$. The theoretical prediction for the scaling coefficient is $B = \frac{c}{2\pi}\sqrt{\frac{A}{L_e}} = 3.98 \pm 0.4$. The reduced chi-squared metric is greater than 1 which suggests the error is underestimated [see Error Analysis section for details].

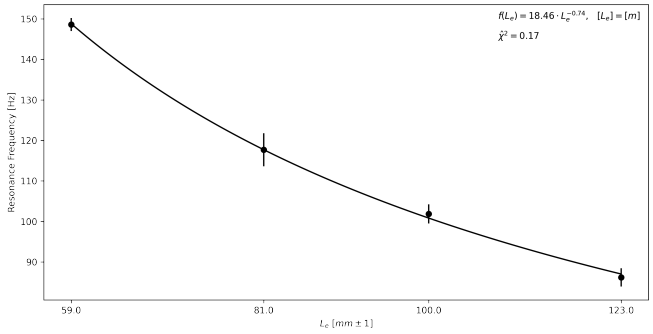

FIG. 8. Resonant frequencies measured for different resonator neck lengths. The curve fit parameters [shown] demonstrate loose agreement with the theoretical power law relationship. The fit exponent is -0.74 which differs from the predicted exponent $b = -1/2$ by approximately 50%. The thoeretical scaling coefficient $B = \frac{c}{2\pi}\sqrt{\frac{A}{V}} = 35.05 \pm 3.53$ also demonstrates disagreement outside the error margin.

spectrogram. SpectrumView supplies a set of discrete frequencies resulting from a uniform Discrete Fourier Transform (DFT) of the audio signal recorded over the time span of one second. The step-size between these frequencies is 7.8125 Hz. Therefore the precision of our frequency measurements is limited to a range of $\pm\Delta\nu = 7.8125/2 \approx 3.9$ Hz.

Next, let us consider how to assess the error of the time-averaging processing step involved in reducing the spectrograms to spectral power distributions. Each time slice of the spectrogram provides a spectral distribution with slight variations from one instant to the next due to noise and other acoustic artifacts. We refer to this as the *statistical error*. By tracking where the peak of the distribution appears at each temporal slice, we effectively perform multiple measurements of the resonant frequency in a single spectrogram. The empirical standard deviation σ_r of the tracked resonant frequency across time gives a characterization of the noise.

To take the precision error and statistical error into account, we model a measurement of the resonant frequency at a single time slice of the spectrogram as a random variable

$$F = X + Y$$

where X and Y are independent random variables. Let X be uniformly distributed about the true the resonant frequency ν_r within a width $2\Delta\nu_r = 7.8125$ corresponding to the frequency step-size in SpectrumView. Concretely,

$$X \sim \text{unif}(\nu_r - \Delta\nu, \nu_r + \Delta\nu)$$

Let Y be zero-mean Gaussian random noise with variance σ_r^2 so,

$$Y \sim \mathcal{N}(0, \sigma_r^2)$$

The measurement error for a single time slice is related to the variance of F. Since X and Y are independent, we have

$$\text{Var}(F) = \text{Var}(X) + \text{Var}(Y)$$

Hence,

$$\text{Var}(F) = \frac{\Delta\nu_r}{3} + \sigma_r^2 \tag{4}$$

Therefore, we take the error of the resonant frequency measurement to be $\sigma_F = \sqrt{\text{Var}(F)}$. This formulation of the error was used to create the error bars shown in Figures 7, 8. It could be argued that because the spectrograms are time-averaged the resonant frequency error should be the standard error $SE = \sigma_F/\sqrt{N_t}$ where N_t is the number of temporal samples in the spectrogram. However, applying this formulation produced error bounds that were unrealistically small. This study errs on the side of caution and instead uses the standard deviation of a single temporal slice σ_F.

C. Q Factor Analysis

The Q factor provides an idea of how much damping there is in the Helmholtz resonator. Qualitatively it expresses how long the resonator will sustain its sound once the experimenter stops blowing air over the opening. It is defined as

$$Q = \frac{\nu_r}{\text{FWHM}(\nu_r)} \tag{5}$$

and relates the width of the resonance peak to the resonance frequency. To extract the Q factors, a gaussian was locally fit to the peaks of each spectral power distribution. An example is shown in Figure 9.

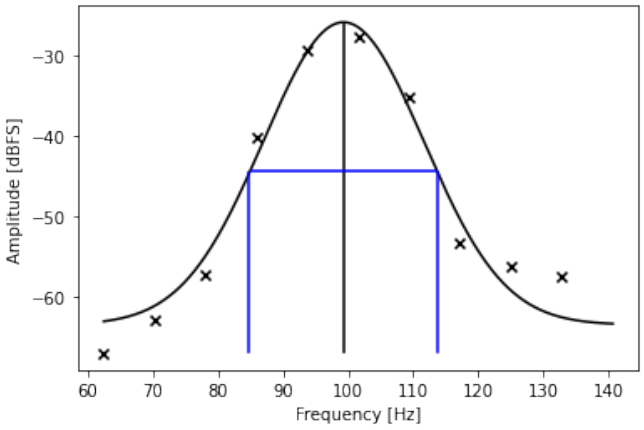

FIG. 9. An illustration of locally fitting a gaussian to a spectral peak at the resonant frequency. Each gaussian was fit using 10 data points centered about the resonance frequency (5 before, 5 after). The FWHM was calculated from the standard deviation of the gaussian as $\sigma\sqrt{8\log 2}$.

As addressed in the section on theory, the Helmholtz resonator can be modeled as a block-spring system. Incorporating damping, the equation of motion for the air column representing the block becomes

$$m\ddot{x} + d\dot{x} + kx = 0 \tag{6}$$

where d is the linear damping coefficient. It is known result in mechanics that the Q factor for the damped harmonic oscillator is

$$Q = \frac{\sqrt{mk}}{d} \tag{7}$$

Therefore, we can interpret low Q-factors to indicate high damping and high Q-factors to indicate low damping.

Figure 10 plots the computed Q factors for each resonance peak for all resonator configurations explored in both experiments (volume and neck length modulation). The choice of a linear fit for the data follows from the linear form of equation 5. Inspecting the slope of the fit, we can extract a measure of the average bandwidth $\delta\omega = \frac{1}{0.02} = 50$ Hz, which is proportional to the damping coefficient d by equation 7.

V. CONCLUSION

An experimental study of the relationship between the resonance frequency of a Helmholtz resonator and two of its geometric parameters is presented. The cavity volume and the neck length of the resonator are found to

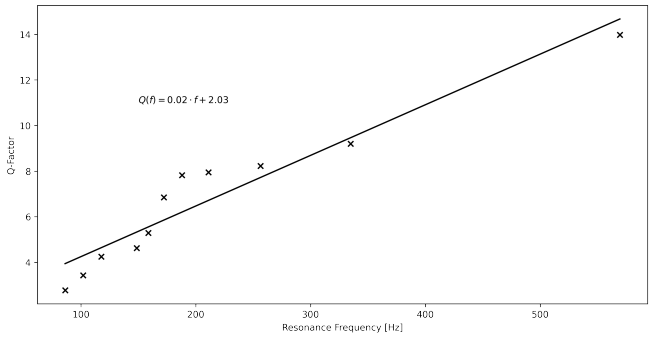

FIG. 10. A linear fit to Q factors of the measured resonance peaks. The slope of the fit is related to the damping of the oscillator.

have an appreciable effect on the resonance frequency. We employ spectral analysis techniques to identify resonance frequencies for different choices of the geometric parameters. A theory of Helmholtz resonators modeled as a block-spring system motivates curve fitting measurements of the resonance frequencies to a power law.

Specifically, our experimental method recovers the cavity volume relationship well with $\nu_r(V) = 4.04 \cdot V^{-0.50}$ closely matching the predicted volume relationship $\nu_r V = 3.98 \cdot V^{-1/2}$. Our experimental method does a poor job of recovering the neck length relationship with $\nu_r(L_e) = 18.46 \cdot {L_e}^{-0.74}$ as opposed to the predicted $\nu_r(L_e) = 35.05 \cdot {L_e}^{-1/2}$.

We posit that the larger discrepancy between experiment and theory in the power law relationship for the neck length can be attributed to at least two factors. First, the copper extensions create an opening diameter (19.8 mm) that is slightly larger than the opening of the standalone Hornitos bottle (18.5 mm). The analysis treated these diameters the same since their respective measurement precisions (±1 mm) contained overlap. However this may have introduced a larger error than anticipated. Second, the correction factor α in equation 3 is highly dependent on the external geometry of the neck. A flanged neck opening, like that of the standalone Hornitos bottle, has a different correction factor than a flangless neck opening, like that of the copper extensions. Our analysis did not account for this difference.

Error analysis of the resonance frequencies distilled from the spectrogram measurements is also provided. We define each resonance frequency is as a compound random variable expressed as a sum of two independent random variables that capture the precision error and the statistical error of the spectrogram measurement. Finally, we characterize the damping of our resonator by fitting Q factors as a function of the resonance frequency via linear regression.

Future studies may consider developing an improved method for neck length modulation that shares the simplicity of stacked cylindrical extensions, but offers finer control over the neck length. This way, more measure-

ments can be collected with a single Helmholtz resonator platform.

ACKNOWLEDGMENTS

The author wishes to acknowledge the support of his colleague Zachary Ross who was an equal partner in collecting data and discussing analytical methods for arriving at the results presented herein. The author also wishes to acknowledge the support and enthusiasm provided by UC Berkeley's Physics 111B professors and Teaching Assistants amidst a trying academic year hampered by a global pandemic.

Appendix A: Derivation of Equation 2

Treating the air as an ideal gas and the resonant process as an adiabatic process, we have $PV^\gamma = c_0 = \text{const.}$

We wish to see how a small change in pressure (drive force) supplied by blowing over the opening changes the volume. Hence differentiating the expression above we have

$$dP = \frac{-c_0\gamma}{V^{\gamma+1}}dV = -\gamma\frac{P}{V}dV$$

We can interpret the small change in volume dV as the amount of air in the neck of the resonator displaced above and below the opening as it oscillates. Then, $dV = Ax$ where x is a small displacement. So we have

$dp = -\gamma\frac{PA}{V}x$

Therefore, the force acting on the mass of air in the neck is simply $F = dPA = -\gamma\frac{PA^2}{V}x$

By Hooke's Law, the force of a spring-mass system is proportional to the displacement $F = -kx$. Therefore, we can identify the equivalent spring constant k in this system to be $k = \gamma\frac{PA^2}{V}$. Inserting this into 1 yields

$$\nu_r = \frac{1}{2\pi}\sqrt{\frac{\gamma PA}{\rho LV}}$$

From the Ideal Gas Law, we have

$$PV = nRT = \left(\frac{\rho V}{m_{air}}\right)RT \Rightarrow \frac{P}{\rho} = \frac{RT}{m_{air}}$$

where ρ is the air density and m_{air} is the mean molecular weight of air. The speed of sound is also known to be

$$c = \sqrt{\frac{\gamma RT}{m_{air}}}$$

Hence, by substituting these new terms into the intermediate expression for ν_r we recover equation 2 up to a correction term in the neck length.

$$\nu_r = \frac{c}{2\pi}\sqrt{\frac{A}{VL}}$$

The correction term has been derived for various circumstances. Interestingly, Lord Rayleigh showed that a resonator with an infinitely long neck and a resonator with no neck converge to the same analytic correction factor $\alpha' = \frac{2}{\pi^{3/2}}$. In this study, we use the analytic correction factor $\alpha' = \frac{8}{3\pi}$ which corresponds to the correction required for a cylindrical neck with a flanged circular opening.

Appendix B: Blackman Window

The Blackman window is a known filter used ubiquitously in audio signal processing. It is similar to a guassian low-pass filter. In the discrete-time regime the window is defined as

$$w[n] = a_0 - a_1\cos\frac{2\pi n}{N} + a_2\cos\frac{4\pi n}{N} \tag{B1}$$

where $a = 0.16$ and

$$a_0 = \frac{1-a}{2} \tag{B2}$$

$$a_1 = \frac{1}{2} \tag{B3}$$

$$a_2 = \frac{a}{2} \tag{B4}$$

[1] B. Rayleigh, *The Theory of Sound*, 2nd ed., Vol. 2 (Dover Publications, New York, 1894).
[2] T. Jonsson, B. D. Chivers, K. R. Brown, F. A. Sarria, M. Walker, and F. Montealegre, Chamber music: an unusual helmholtz resonator for song amplification in a neotropical bush-cricket (orthoptera, tettigoniidae), Journal of Experimental Biology **220** (2017).
[3] M. H. Khairuddin, M. F. M. Said, A. A. Dahlan, and K. A. Kadir, Review on resonator and muffler configuration acoustics, Archives of Acoustics **43**, 369 (2018).
[4] M. Dannemann, M. Kucher, E. Kunze, N. Modler, K. Knobloch, L. Enghardt, E. Sarradj, and K. Höschler,

Experimental study of advanced helmholtz resonator liners with increased acoustic performance by utilising material damping effects, Applied Sciences **8**, 1923 (2018).

[5] Window functions, Wikimedia Foundation (2021), available at `https://en.wikipedia.org/wiki/Window_function`.

[6] H. G. Dosch and M. Hauck, The helmholtz resonator revisited, European Journal of Physics. **39**, 19 (2018).